

FIG. 1: v vs F characteristics for $\gamma = 0.2$. Data for $T = 0.003$ obtained for $L_{xy} = 40$ are also included (light-blue squares). Inset: data for zero temperature. Error bars are smaller than the size of symbols.

posed to be uniform. Periodic boundary conditions are put in all the three directions. The results shown below are for $N_v = 180$, $N_p = 900$, $N_z = 20$, $L_{xy} = 30$. The magnetic field is roughly $B \approx 100$ G if we take $a_b = 2000$ Å [21]. The equation is integrated by the 2nd order Runge-Kutta algorithm with $\Delta t = 0.002$ – 0.01 . All data presented below are the average over 10 samples with different randomly distributed pins. Fixing the magnetic field, we have performed simulations for $L_{xy} = 20$ and 40 , and make sure that finite-size effects are negligible to the main, universal results. For pinning strength, we choose $\gamma = 0.2$ and $\gamma = 0.05$, for which the maximum curvatures of the pinning potential are 4.87 and 1.22 , above and below the tilt modulus of the flux lines $C \approx 1.47$; they are therefore expected to fall into the strong and weak collective pinning regimes respectively [22, 23].

Strong pinning { Let us begin with the strong pinning case of $\gamma = 0.2$. The equilibrium state is a pinned solid (VG) as random as liquid seen from the structure factor. The v vs F characteristics at low temperatures are depicted in Fig. 1 ($T = 0$ in inset). A continuous depinning transition is observed at $T = 0$ with a unique depinning force [24], which can be described by $v \propto A(F - F_{c0})^1$ with $F_{c0} \approx 0.231$ – 0.002 and $A \approx 0.74$ – 0.02 . For $0 < T < 0.0005$, upward-convex v vs F characteristics are observed down to F_{c0} ; below F_{c0} there is an extremely small tail which is hard to see in the present scale.

The sharp depinning transition is clearly rounded by finite temperatures. In order to explore the critical properties of the v vs F characteristics at finite temperatures, we postulate the following scaling ansatz [25, 26, 27]

$$v(T; F) = T^{1/\beta} S((F - F_{c0})/T^{1/\beta}) \quad (2)$$

with $f = (F - F_{c0})/T^{1/\beta}$ [28] and the scaling function $S(x)$

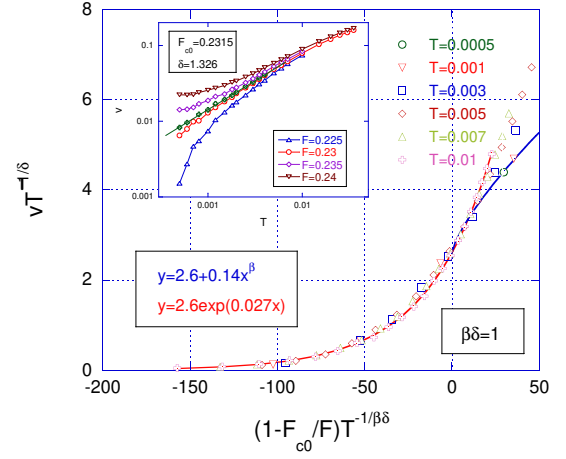


FIG. 2: Scaling plot for the data in Fig. 1. Inset: Temperature dependence of velocity for several forces around F_{c0} .

regular at $x = 0$ and $S(x) \sim x$ as $x \rightarrow +1$.

The critical force can be determined using the property $v(T; F = F_{c0}) = S(0)T^{1/\beta}$ implied in Eq. (2) (see also [29]). As shown in the inset of Fig. 2, we evaluate $F_{c0} = 0.2315$ – 0.0013 , and meanwhile from the slope $1/\beta = 0.754$ – 0.010 . We then perform the scaling plot using the scaled variables $vT^{1/\beta}$ and $(1 - F_{c0}/F)T^{1/\beta}$; the best collapsing of data to a single scaling curve is achieved when $1/\beta = 0.754$, thus determining the exponent β . The values of F_{c0} and β estimated from data at finite temperatures via the scaling analysis are consistent with those derived from $T = 0$, which can be taken as an evidence for the existence of scaling. Fitting the scaling curve, we obtain $S(x) = 0.14x + 2.6$ for $x > 0$ and $S(x) = 2.6\exp(0.027x)$ for $x < 0$; the former covers the continuous depinning transition at $T = 0$; the latter, combined with the relation $\beta\delta = 1$, indicates that the motion at low temperatures and forces below F_{c0} is well described by the Arrhenius law, and that the energy barrier disappears linearly when the force is ramped up to F_{c0} ; the bare energy barrier is $U_c = 0.027$.

The same exponents and similar scaling behaviors are available for $\gamma = 0.05$; therefore, the above properties are universal for strong pinning case. The creep law derived above confirms the a priori assumption in the Anderson-Kim theory [30], and coincides with the FRG results in Ref. [31] for a domain wall ($N = 1$). Our results are also consistent with Ref. [29] provided $\beta = 1$.

Deviations from the scaling curve are observed for (a) $F_{c0} = 2 < F < F_{c0}$ at $T \approx 0.015$, $U_c = 2$, due to extra thermal deformation of flux-line lattice; (b) $F < F_{c0} = 2$ which may be governed by the zero-force limit; and (c) $F < F_{c0}$ the flux-flow regime.

Weak collective pinning { We have performed the same simulations for $\gamma = 0.05$, which falls into the weak collective pinning regime. The equilibrium state is a BrG, with the melting temperature $T_m \approx 0.077$ above which the quasi long-range order is suppressed by thermal fluctua-

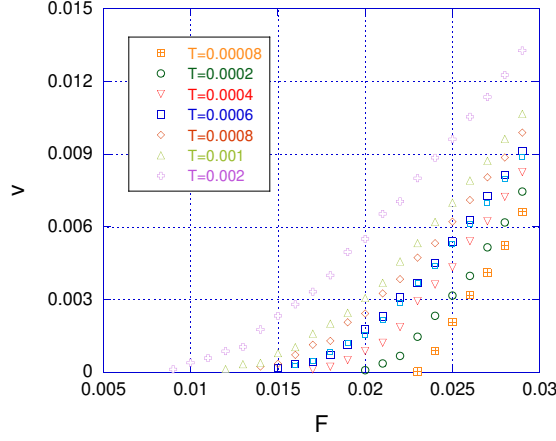


FIG. 3: v vs F characteristics for $\alpha = 0.05$. Data for $T = 0.0006$ obtained for $L_{xy} = 40$ (light-blue squares).

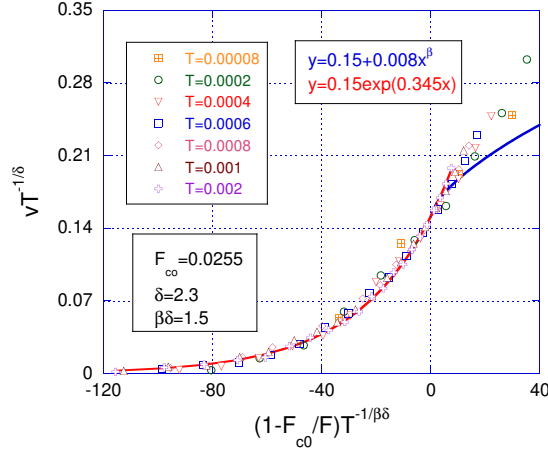


FIG. 4: Scaling plot for data in Fig. 3.

tions. Looking at the velocity-velocity correlation function, we find in this case that the moving system shows good temporal and spatial orders characterized by Bragg peaks [32, 33] (No moving smectic [34] was observed for the present parameters.) The v vs F characteristics are shown in Fig. 3, where similar to the strong pinning case, a sharp crossover between the depinning and creep motion takes place at F_{c0} for $0 < T \leq 0.00008$. The scaling plot is depicted in Fig. 4. The exponents are estimated as $\delta = 2.3 \pm 0.1$ and $\beta\delta = 0.65 \pm 0.01$, which are different from those for strong pinning case. The product of the two exponents $\beta\delta = 3 \pm 2$ deviates from unity, indicating a nonlinear scaling relation between temperature and force deviation from F_{c0} .

Nonlinear scaling relations have been found in CDW systems [26]. This behavior can be captured by an effective potential of linear and cubic terms of displacement, with a small energy barrier [12, 26]. The linear scaling relation observed for strong pinning force corresponds to an

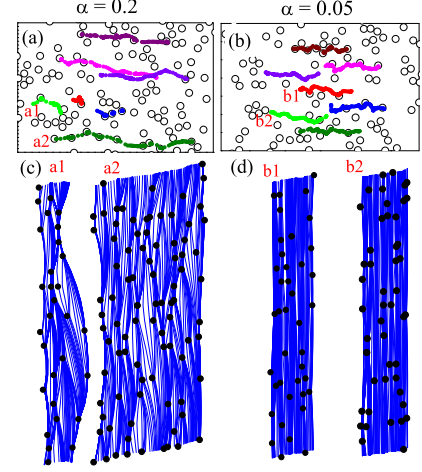


FIG. 5: Vortex motions at $T = 0$. (a) and (b): Trajectories of 7 nearest-neighbor vortices on one layer for $\alpha = 0.2$ at $F = 0.024$ and $\alpha = 0.05$ at $F = 0.027$ respectively. (c) and (d): Trajectories of the two flux lines indicated in (a) and (b). The total times are 330 for $\alpha = 0.2$, and 1200 for $\alpha = 0.05$, such that flux lines in both systems move roughly the same distance $4 \pm 1.7a_0$ in average. Open circles in (a) and (b) represent the positions of pins, while the filled circles in (c) and (d) represent pins that pin the flux lines.

effective potential of linear, quadratic and quartic terms of displacement, with a large energy barrier [35]. It is observed in our simulations that the system with weak bare pinning strength experiences smaller energy barriers compared with that of strong bare pinning strength, even at the same relative force-deviation from the critical values; an analytic derivation of the effective energy barrier, however, is not an easy task [12]. While a full picture remains to be developed, we notice that, first, vortex motions in nucleation processes in first-order phase transitions: the weak/strong pinning case corresponds to a system located at the spinodal/coexistence curve [35]; secondly, under weak and strong pinning vortices behave similarly to CDW [26] and domain wall [31] respectively, due to the different ranges of correlation.

The scaling curve in Fig. 4 is fitted well by $S(x) = 0.15 \exp(0.345x)$, which, with the nonlinear scaling variable, indicates a non-Arrhenius creep motion for the weak pinning case. To the best of our knowledge, this behavior has not been reported so far. On a phenomenological level, it can be captured with an appropriate correlator of energy barriers [36].

"Microscopic" vortex motion { We have examined the microscopic motions of flux lines. As detailed in Fig. 5 for forces slightly above F_{c0} and at zero temperature (similar results have been obtained for $F < F_{c0}$ at finite temperatures), flux lines in the weak pinning case move homogeneously in an intermediate time scale, which guarantees the moving BrG (m BrG) order [33]; flux lines under strong pinning move in an inhomogeneous way, and thus additional dislocations are induced during the motion.

Even for the case of mB/g , velocity fluctuates for time being and between different vortices, as can be seen in Fig. 5d. Namely in a shorter time scale, the motion of vortices in weak pinning case is also random: Flux lines exhibit an intermittent pattern of motion, i.e. a portion of flux lines move while others are almost motionless at a given time window, and in the next time window, similar situation occurs with the moving vortices found in different regions. The motion of the total system is thus an accumulation of individual, random movements, in which creep events dominate and the random pinning plays an essential role. As shown in Figs. 5c and d the shape of vortex lines upon depinning depends on pin strength [23].

Discussions { The strong pinning $\beta = 0.2$ and weak collective pinning $\beta = 0.05$ according to the Labusch criterion [22, 23] result in vortex glass and Bragg glass respectively. But generally the Labusch criterion does not coincide with the phase boundary of Bragg glass. Further study is expected to resolve this point in detail.

As can be seen in Figs. 5a and b, during the creep motion vortices displace frequently into the direction transverse to the force and the averaged velocity. In this way a bypath of lower energy can be found which assists vortices to avoid otherwise high energy barriers. This

may affect the averaged velocity significantly since the time spent in large energy barriers is huge, and is to be taken into account carefully in theoretical treatments.

Beside the genuine, zero-temperature depinning transition, we observe a quite steep crossover between the depinning and creep motions at low temperatures ($T = 0.0005$ for $\beta = 0.2$ and $T = 0.00008$ for $\beta = 0.05$). The velocity tail below the crossover is very small as such it looked like a phase transition in simulations (and perhaps also in experiments). The crossover, however, loses its sharpness when temperature increases but still far below the melting temperature, which might be not quite consistent with experimental phase boundary $H_g(T)$ [14]. The possibility of a transition (or sharp crossover) between the depinning and flux flow regimes remains to be investigated within the present formalism, taking into account the shaking magnetic field.

Acknowledgements { We are pleased to acknowledge T. Nattermann, D. Genshkenbein, G. Blatter, B. Rosenstein, V. Vinokur and D. P. Li for discussions. Calculations were performed on SR11000 (HITACHI) in NIMS. X. H. is supported by Grant-in-Aid for Scientific Research (C) No. 18540360 of JSPS, and project ITSNEM of China Academy of Science.

-
- [1] T. Nattermann, Phys. Rev. Lett. 64, 2454 (1990).
 - [2] T. Giamarchi and P. Le Doussal, Phys. Rev. Lett. 72, 1530 (1994); Phys. Rev. B 52, 242 (1995).
 - [3] D. S. Fisher, M. P. A. Fisher and D. A. Huse, Phys. Rev. B 43, 130 (1991).
 - [4] A. I. Larkin and Yu. N. Ovchinnikov, J. Low Temp. Phys. 34, 409 (1979).
 - [5] L. B. Ioannidis and V. M. Vinokur, J. Phys. C 20, 6149 (1987).
 - [6] T. Nattermann, Europhys. Lett. 4, 1241 (1987).
 - [7] M. V. Feigel'man et al., Phys. Rev. Lett. 63, 2303 (1989).
 - [8] G. Blatter et al., Rev. Mod. Phys. 66, 1125 (1994);
 - [9] P. Chauve, T. Giamarchi, P. Le Doussal, Phys. Rev. B 62, 6241 (2000).
 - [10] T. Giamarchi and S. Bhattacharya, High Magnetic Fields: Applications in Condensed Matter Physics, Spectroscopy (Springer, New York, 2002), p. 314.
 - [11] T. Nattermann and S. Scheidl, Adv. Phys. 49, 607 (2000).
 - [12] S. B. Razovskii and T. Nattermann, Adv. Phys. 53, 177 (2004).
 - [13] A. B. Kolton, A. Rosso and T. Giamarchi, Phys. Rev. Lett. 94, 047002 (2005).
 - [14] H. Beidenkopf et al., Phys. Rev. Lett. 95, 257004 (2005).
 - [15] D. P. Li and B. Rosenstein, cond-mat/0411096.
 - [16] S. Ryu et al., Phys. Rev. Lett. 68, 710 (1992).
 - [17] C. Reichhardt, C. J. Olson and F. N. Nori, Phys. Rev. Lett. 78, 2648 (1996).
 - [18] A. van Otterlo, R. T. Scalettar, and G. T. Zimanyi, Phys. Rev. Lett. 81, 1497 (1998).
 - [19] E. Olive et al., Phys. Rev. Lett. 91, 37005 (2003).
 - [20] Q. H. Chen and X. Hu, Phys. Rev. Lett. 90, 117005 (2003); The work clarifies the regime of current and temperature where vortex loops are excited, which is beyond the application of the present model.
 - [21] E. Zeldov et al., Nature 375, 373 (1995).
 - [22] R. Labusch, Cryst. Lattice Defects, 1, 1 (1969).
 - [23] G. Blatter, V. B. Geshkenbein and J. A. G. Koopeann, Phys. Rev. Lett. 92, 67009 (2004).
 - [24] A. A. Lan.Middleton, Phys. Rev. Lett. 68, 670 (1992). The theory works for the present case but cannot be proved explicitly.
 - [25] D. S. Fisher, Phys. Rev. Lett. 50, 1486 (1983); *ibid* Phys. Rev. B 31, 1396 (1985).
 - [26] A. A. Lan.Middleton, Phys. Rev. B 45, 9465 (1992).
 - [27] L. Roters et al., Phys. Rev. B 60, 5202 (1999).
 - [28] The usually adopted quantity $f^0 = 1 - F/F_{c0}$ gives the same exponents, but the scaling regime is much narrower.
 - [29] T. Nattermann, V. Pokrovsky, and V. M. Vinokur, Phys. Rev. Lett. 87, 197005 (2001).
 - [30] P. W. Anderson and Y. B. Kim, Rev. Mod. Phys. 36, 39 (1964).
 - [31] M. Müller, D. A. Gorokhov, G. Blatter, Phys. Rev. B 63, 184305 (2001).
 - [32] L. Balents and M. P. A. Fisher, Phys. Rev. Lett. 75, 4270 (1995).
 - [33] T. Giamarchi and P. Le Doussal, Phys. Rev. Lett. 76, 3408 (1996); P. Le Doussal and T. Giamarchi, Phys. Rev. B 57, 11356 (1998).
 - [34] L. Balents, M. Cristina, and L. Radzihovsky, Phys. Rev. Lett. 78, 751 (1997); *ibid* Phys. Rev. B 57, 7705 (1998).
 - [35] Y. Sang, M. Dube, and M. Grant, Phys. Rev. Lett. 87, 174301 (2001).
 - [36] P. Le Doussal and V. M. Vinokur, Physica C, 254, 63 (1995).